JOURNAL OF COMPUTATIONAL PHYSICS 67, 73 90 (1986)

# Numerical Solution of Two-Dimensional Stokes Equations for Flow with Particles in a Channel of Arbitrary Shape Using Boundary-Conforming Coordinates

A. S. DVINSKY

*Creare Incorporated, Hanover, New Hampshire 03755*

AND

A. S. POPEL

*Department of Biomedical Engineering, Johns Hopkins University, Baltimore, Maryland 21205*

Received August 21, 1985; revised January 17, 1986

A numerical scheme is proposed for the solution of two-dimensional Stokes equations in a multiconnected domain. The numerical procedure is based on a finite-difference solution of the governing equations in general curvilinear coordinates. Several examples of calculations are presented for a circular particle in a plane channel; the results are compared to known analytical solutions. The proposed scheme is applicable to the cases of flow around multiple stationary or moving particles of arbitrary shape in channels of arbitrary shape. 

## INTRODUCTION

A numerical procedure is developed for the solution of two-dimensional quasi-steady creeping flow equations for an incompressible fluid in a general multiconnected domain. A particular application discussed in the paper is the flow around a particle or a group of particles in a channel of arbitrary shape. The problem of slow motion of rigid particles in narrow channels is important in a variety of engineering and biomedical applications. For example, it can serve as a model for the motion of binary mixtures through porous beds in chemical engineering or for the motion of red blood cells and leucocytes in microvessels. The knowledge of flow through individual channels can subsequently be utilized in constructing flow in networks. Despite its significance only a few investigators have applied numerical methods to treat the problems of particle motion in channels or tubes. A finite element solution for the analysis of axisymmetric creeping flow around an infinite train of equally spaced particles in a round tube was developed in [1]. A similar axisymmetric problem was treated in [2] by a finite-difference method; the Marker-and-Cell (MAC) method was employed for finite Reynolds number flows and a modified



0021-9991/86 $3.00

method (MACRL) [3] was applied in the case of low Reynolds number flow. The authors reported good agreement with analytical solutions [4, 5] for a train of spherical particles in axisymmetric creeping flow. Recently, collocation solutions were obtained for axisymmetric and nonaxisymmetric motion of a spherical particle between two parallel planes in Poiseuille and Couette flows, and in the case of sedimentation [6, 7, 8].

Few results are available for the problem of two-dimensional flow with particles in a channel. The results are limited to analytical solutions in the form of asymptotic expansions for the case of plane channel and axisymmetrically situated circular particle. No solutions have been found for more general cases. The present work is an attempt to fill this gap. The finite-difference method developed here for the solution of Stokes' equations in vorticity-stream function form incorporates numerical generation of boundary-conforming coordinate systems (e.g., [9]). The boundary-conforming coordinate systems are generated as solutions of a set of two elliptic quasilinear partial differential equations. The use of numerically generated boundary-conforming coordinates is an important element of the proposed procedure; it eliminates error due to interpolation at the curvilinear boundaries, allows the resolution of high gradients in narrow gaps, and significantly facilitates computations and programming due to "matrix" arrangement of grid functions.

The following sections describe the Stokes equations for incompressible, two-dimensional, quasisteady flow in a curvilinear boundary-conforming coordinate system; the analytic boundary conditions; the scheme for calculating the hydrodynamic force and torque exerted by the fluid on the suspended particle; and the numerical procedure for solving the equations together with the computational boundary conditions.

## Governing Equations

The stream function, $\psi'$, and vorticity, $\omega'$, are defined as follows:

$$u' = \frac{\partial \psi'}{\partial y'}, \qquad v' = -\frac{\partial \psi'}{\partial x'}, \tag{1}$$

$$\omega' = \frac{\partial v'}{\partial x'} - \frac{\partial u'}{\partial y'}. \tag{2}$$

Let $H$ be a characteristic length, and $U$ be a characteristic velocity of the problem. Dimensionless variables are introduced by the relationships

$$x = \frac{x'}{H}, \qquad y = \frac{y'}{H}, \qquad u = \frac{u'}{U}, \qquad v = \frac{v'}{U},$$
$$p = \frac{p'H}{\mu U}, \qquad \psi = \frac{\psi'}{UH}, \qquad \omega = \frac{\omega'}{U} H. \tag{3}$$

Using (1) (3) the dimensionless Stokes equations in vorticity-stream function form (e.g., [7]) are

$$\omega_{xx} + \omega_{yy} = 0, \tag{4}$$

$$\psi_{xx} + \psi_{yy} = -\omega, \tag{5}$$

where the indices $x$, $y$ denote partial derivatives with respect to the corresponding variable. The derivatives of pressure can be expressed in terms of the derivatives of vorticity

$$\frac{\partial p}{\partial x} = -\frac{\partial \omega}{\partial y}, \qquad \frac{\partial p}{\partial y} = \frac{\partial \omega}{\partial x}. \tag{6}$$

Consider a coordinate transformation

$$x = x(\xi, \eta), \qquad y = y(\xi, \eta) \tag{7}$$

defined as a solution of two elliptic quasilinear partial differential equations [9],

$$\begin{aligned} g_{22}x_{\xi\xi} - 2g_{12}x_{\xi\eta} + g_{11}x_{\eta\eta} &= -G^2(Px_\xi + Qx_\eta), \\ g_{22}y_{\xi\xi} - 2g_{12}y_{\xi\eta} + g_{11}y_{\eta\eta} &= -G^2(Py_\xi + Qy_\eta), \end{aligned} \tag{8}$$

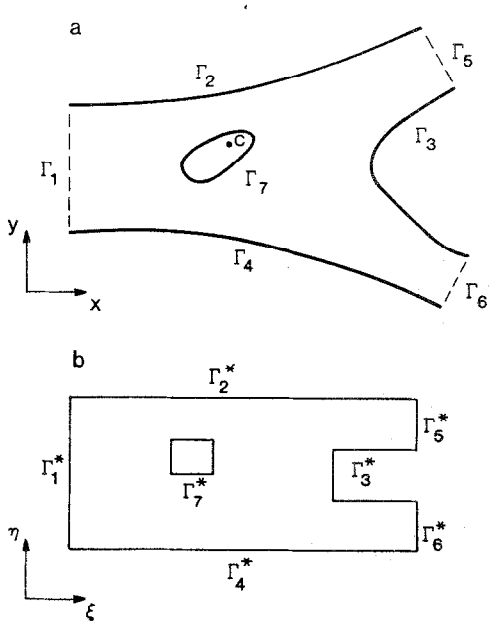


FIG. 1. An example of region transformation.

where

$$g_{11} = x_\xi^2 + y_\xi^2, \qquad g_{12} = x_\xi x_\eta + y_\xi y_\eta, \qquad g_{22} = x_\eta^2 + y_\eta^2. \tag{9}$$

$G$ is the Jacobian of the transformation

$$G = x_\xi y_\eta - x_\eta y_\xi \tag{10}$$

and $P = P(\xi, \eta)$ and $Q = Q(\xi, \eta)$ are functions chosen to control the spacing of coordinate lines in the $x$–$y$ plane.

The mapping (7) is utilized to transform the flow domain with generalized curvilinear boundaries into a domain with rectilinear boundaries on the "computational" plane $\xi$–$\eta$ as illustrated in Fig. 1. The system of equations [11] is solved by an SOR method (see, e.g., [10]). An example of the transformation for a circular particle in a bifurcating channel is shown in Fig. 2; the lines in the physical $x$–$y$ plane correspond to lines $\xi = \text{const.}$ and $\eta = \text{const.}$ in the computational plane.

Equations (4) and (5) are now transformed to the new coordinates

$$\nabla_{\xi\eta}^2 \omega \equiv G^{-2}[g_{22}\omega_{\xi\xi} - 2g_{12}\omega_{\xi\eta} + g_{11}\omega_{\eta\eta} + G^2 P\omega_\xi + G^2 Q\omega_\eta] = 0, \tag{11}$$

$$\nabla_{\xi\eta}^2 \psi = -\omega. \tag{12}$$

Equations (6) become

$$p_\xi = G^{-1}(g_{12}\omega_\xi - g_{11}\omega_\eta), \qquad p_\eta = G^{-1}(g_{22}\omega_\xi - g_{12}\omega_\eta). \tag{13}$$

Here the indices $\xi$ and $\eta$ denote differentiation with respect to the corresponding variable.

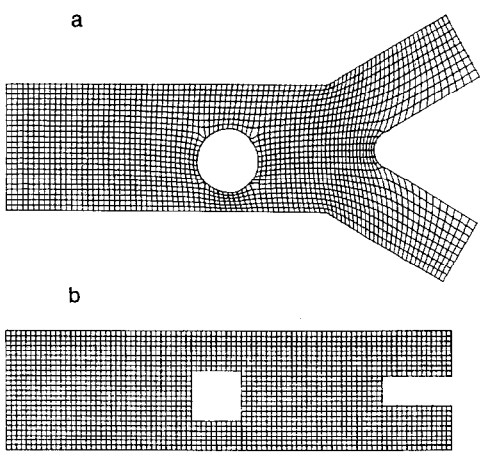


FIG. 2. Coordinate system (a) for the mapping shown below (b).

## Boundary Conditions

Consider a channel of an arbitrary shape, for example as shown in Fig. 1. For the sake of brevity, in the following formulations, a single rigid particle of an arbitrary shape with the boundary $\Gamma_p$ will be considered; however, all procedures described below are easily extendable to the case of $N$ particles. The boundary of the channel, $\Gamma$, consists of the solid part, $\Gamma_s$, and the fluid part, $\Gamma_f$ (channel inlets and outlets). The fluid velocity is assumed to be given on both $\Gamma_s$ and $\Gamma_f$. Additionally, the translational velocity of a point $c$ within the particle, $U_c$, and the angular velocity of the particle $\Omega$, are specified. Thus, the velocity distribution on the particle boundary, $\Gamma_p$, is given by

$$\begin{aligned} u &= U_c - \Omega(y - y_c), \\ v &= V_c + \Omega(x - x_c), \end{aligned} \tag{14}$$

where $(U_c, V_c)$ are the cartesian velocity components of the point $c$, and $(x_c, y_c)$ are its coordinates.

Equations (4) and (5) are equivalent to a single biharmonic equation for the stream function. It is more convenient at this point to formulate boundary conditions for the stream function because there are no "natural" boundary conditions for the vorticity. A possible way to pose the boundary value problem for a biharmonic equation is to specify the function and its normal derivative on the boundaries (e.g., [11]). Using (1) one can determine the stream function at the channel boundary

$$\psi = \psi_A + \int_{\Gamma} (-v dx + u dy), \tag{15}$$

where $\psi_A$ is an arbitrarily specified value of the stream function at a point $A$ on the boundary, and $u$ and $v$ are given cartesian velocity components on the boundary. Similarly,

$$\psi = C + \int_{\Gamma_p} (-v dx + u dy), \tag{16}$$

where $C$ is an unknown constant that will be determined later, and the velocity components $u$ and $v$ are given by (14).

Let $\bar{n}$ be a unit vector normal to the boundary and directed into the fluid; its angle with the positive $x$ axis is denoted by $\alpha$. At the boundary

$$\frac{\partial \psi}{\partial n} = -v \cos \alpha + u \sin \alpha. \tag{17}$$

The biharmonic equation for $\psi$ with boundary conditions (15)–(17) has a unique

solution for each value of the constant $C$ in (16) if the boundary and the velocity distribution are sufficiently smooth [11]. Once the stream function is known, the vorticity can be found from (5) and the pressure distribution from (6).

Consider a contour $L_p$ enclosing the particle as shown in Fig. 3a and calculate along this contour:

$$q = \int_{L_p} dp = \int_{B_-}^{B_+} dp. \tag{18}$$

Obviously, the pressure $p$ must be a single-valued function of the position, thus $q$ must be equal to zero. This condition is not satisfied automatically, however, for an arbitrary choice of $C$. If $C$ in (16) is considered as a parameter then, due to the linearity of the problem, $q$ in (18) must be a linear function of $C$ for a given contour $L_p$,

$$q = \lambda_1 C + \lambda_2. \tag{19}$$

Thus, an additional condition $q = 0$ determines the parameter $C$ in (16).

The numerical scheme described below deals with two coupled second order partial differential equations (4) and (5) for vorticity and stream function rather than

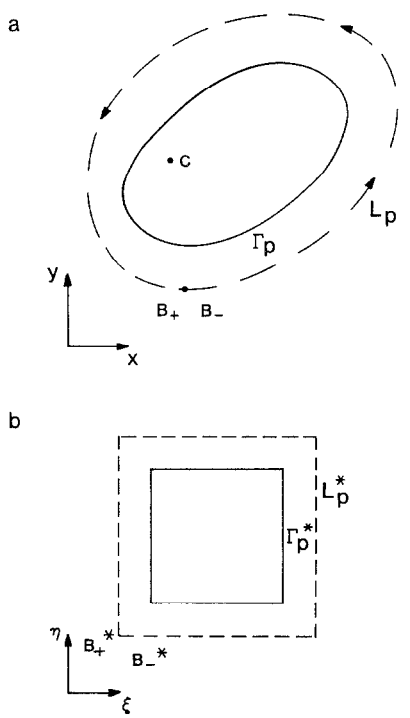


FIG. 3. Integration contour.

with a single biharmonic equation. This approach makes it necessary to formulate computational boundary conditions for vorticity in addition to the conditions discussed above; these additional conditions will be described below as a part of the numerical scheme.

## Calculation of the Force and Torque on the Particle

Assuming that the stream function, vorticity, and pressure fields in the fluid are known, and therefore the velocity components can be calculated, one can find the force and torque exerted on the particle. In the transformed coordinates introduced earlier, the force and torque are given by

$$F_1 = \int (py_\xi - \omega x_\xi)\, d\xi + \int (py_\eta - \omega x_\eta)\, d\eta, \tag{20}$$

$$F_2 = \int (px_\xi - \omega y_\xi)\, d\xi + \int (px_\eta - \omega y_\eta)\, d\eta, \tag{21}$$

$$\begin{aligned} T = &-\int \{[px + (2\Omega - \omega)\, y]\, x_\xi + [py - (2\Omega - \omega)\, x]\, y_\xi\}\, d\xi \\ &-\int \{[px + (2\Omega - \omega)\, y]\, x_\eta + [py - (2\Omega - \omega)\, x]\, y_\eta\}\, d\eta, \end{aligned} \tag{22}$$

where

$$F_1 = \frac{F_1'}{\mu U}, \qquad F_2 = \frac{F_2'}{\mu U}, \qquad T = \frac{T'H}{\mu U}. \tag{23}$$

It can be shown that the integrals (20) and (21) can be computed over any closed contour containing particle [12]. Recognizing that shifting the contour of integration from the particle surface presents significant computational advantages the integrals in (20) and (21) are calculated along $L_p^*$ (Fig. 3b). The integral in (22) is computed along $\Gamma_p^*$.

Because the equations of motion are linear, the force and torque on the particle can be presented as a sum of the following terms:

(a) a translational part due to the particle motion with velocity $U_c$ with the fluid velocity being zero at all other boundaries,

(b) a rotational part due to the particle rotation with angular velocity $\Omega$ with the fluid velocity being zero at all other boundaries, and

(c) a part due to the motion of fluid at the boundaries of the region while the particle is at rest.

Thus the force and torque exerted by the fluid on the particle can be expressed as a sum

$$\begin{pmatrix} F_1 \\ F_2 \\ T \end{pmatrix} = \begin{pmatrix} A_{11} & A_{12} & A_{13} \\ A_{21} & A_{22} & A_{23} \\ A_{31} & A_{32} & A_{33} \end{pmatrix} \begin{pmatrix} U_c \\ V_c \\ \Omega \end{pmatrix} + \begin{pmatrix} F_{10} \\ F_{20} \\ T_0 \end{pmatrix}, \tag{24}$$

where the elements of the resistance matrix $A_{ij}$ are functions of the geometry of the problem. It has been shown [9, 13] that under certain conditions, which are satisfied in the present case, the matrix $A_{ij}$ is symmetric.

In many cases one is interested in the velocities of a free particle when there are no external forces applied to it except for the hydrodynamic forces. In accordance with the assumption of quasisteady flow made above, one can also assume that the motion of the particle is quasistatic, i.e., the sum of forces acting on the particle is zero. The relationship (24) can then be considered as a set of linear algebraic equations with respect to the velocities $U_c$, $V_c$, and $\Omega$ provided that the coefficients in (24) are known. To determine the coefficients, the forces and torque on a quiescent particle in a moving fluid are first calculated, yielding the last column in (24). To determine the rest of the coefficients, we calculate the forces and torque for three different sets of velocities $(U_{c1}, V_{c1}, \Omega_1)$, $(U_{c2}, V_{c2}, \Omega_2)$, and $(U_{c3}, V_{c3}, \Omega_3)$ and solve the set of equations (24) for the nine coefficients $A_{ij}$ $(i, j = 1, 2, 3)$. In the present calculations the following sets were considered: $(U_{c1}, 0, 0)$ $(0, V_{c2}, 0)$, and $(0, 0, \Omega_3)$. It should be noted that, theoretically, there are only six independent coefficients in the matrix $A_{ij}$ due to its symmetry. Therefore, it appears that only six equations generated by two sets of velocities are sufficient for their determination. In reality, however, the forces and torques are calculated with certain numerical error. As a result, the computed matrix is not perfectly symmetric and it is necessary to determine all nine coefficients of the matrix. Thus, to determine the free particle velocities, the fluid mechanical problem for flow around a particle has to be solved four times with different specified particle velocities.

In the case where there is an external force $F_{1e}$, $F_{2e}$, and/or torque, $T_e$, exerted on the particle (e.g., due to buoyancy) the equations of particle quasiequilibrium become

$$F_1 = F_e, \qquad F_2 = F_{2e}, \qquad T = T_e, \tag{25}$$

where the left-hand sides are given by (24). The coefficients $A_{ij}$ are independent of the external forces, and therefore can be determined from the procedure described above. Solving (25) for $U_c$, $V_c$, and $\Omega$ yields the velocities of the particle in the case of a constrained motion.

Once the velocities of the particle are known, the trajectory of the particle, $x_c(t)$ and $y_c(t)$, and the angle, $\alpha(t)$, between a fixed line in the particle and the positive $x$ axis, can be determined by integrating the equations

$$\frac{dx_c}{dt} = U_c, \qquad \frac{dy_c}{dt} = V_c, \qquad \frac{d\alpha}{dt} = \Omega, \tag{26}$$

where $U_c$, $V_c$, and $\Omega$ are function of $x_c$, $y_c$, and $\alpha$. Initial conditions

$$x_c(0) = x_{c0}, \qquad y_c(0) = y_{c0}, \qquad \alpha(0) = \alpha_0 \tag{27}$$

define the initial location and orientation of the particle.

In the following section the numerical implementation of the outlined solution algorithm will be described.

## Finite-Difference Equations and Numerical Solution

In this section the numerical algorithm for the fluid mechanical problem is formulated. The system of Stokes equations (11) and (12) in the vorticity-stream function form in the transformed (computational) plane is approximated using second order central finite-difference formulae

$$\begin{aligned} L_{i,j}\psi \equiv\ & g_{22}(\psi_{i+1,j} - 2\psi_{i,j} + \psi_{i-1,j}) - 2g_{12}(\psi_{i+1,j-1} - \psi_{i+1,j-1} - \psi_{i-1,j+1} \\ & + \psi_{i-1,j-1})/4 + g_{11}(\psi_{i,j+1} - 2\psi_{i,j} + \psi_{i,j-1}) + PG^2(\psi_{i+1,j} - \psi_{i-1,j})/2 \\ & + QG^2(\psi_{i,j+1} - \psi_{i,j-1})/2 = -G^2\omega_{i,j}, \end{aligned} \tag{28}$$

$$L_{i,j}\omega = 0, \tag{29}$$

where $L_{i,j}$ is a finite-difference operator at a point $\xi = i$, $\eta = j$. The coefficients $g_{11}$, $g_{12}$, $g_{22}$, $P$, $Q$, and Jacobian $G$, given by (8)–(10), are evaluated at the point $(i, j)$.

It is necessary when solving the difference equations (28), (29) to have values of both the stream function and vorticity at the boundary. In a preceding section, we have described how the stream function can be specified at the channel boundary using (15), and at the particle boundary using (16) up to an unknown constant $C$. The numerical procedure for determining the constant $C$ will be described later in this section.

The value of vorticity at the boundary is obtained from (28) and the no-slip, no-permeability conditions at the wall are obtained as follows. First, the derivatives of the stream function are expressed via velocity components

$$\begin{aligned} \psi_\xi &= uy_\xi - vx_\xi, \\ \psi_\eta &= uy_\eta - vx_\eta. \end{aligned} \tag{30}$$

The derivatives of the stream function (30) are discretized using an expression of third order accuracy

$$(\psi_\eta)_j = \frac{2\psi_{j+1} + 3\psi_j - 6\psi_{j-1} + \psi_{j-2}}{2}. \tag{31}$$

Using Eq. (28) (with $P=Q=0$ for brevity) and substituting for points outside of the domain one can express the vorticity at the boundary shown in Fig. 4a,

$$\begin{aligned}\omega_{i,j} = -\{&g_{22}(\psi_{i+1,j} - 2\psi_{i,j} + \psi_{i-1,j}) - g_{12}[3(\psi_\eta)_{i+1,j} - 3(\psi_\eta)_{i-1,j} \\ &+ 2(\psi_{i+1,j-1} - \psi_{i-1,j-1}) + 3/2(\psi_{i-1,j} - \psi_{i+1,j}) \\ &+ (\psi_{i-1,j-2} - \psi_{i+1,j-2})/2]/2 + g_{11}[3(\psi_\eta)_{i,j} + 4\psi_{i,j-1} - 7/2\psi_{i,j} \\ &- \tfrac{1}{2}\psi_{i,j-2}]\}/G^2,\end{aligned} \tag{32}$$

where the derivative $\psi_\eta$ is calculated with the help of (30). The resulting expression (32) is accurate to second order. However, if instead of (31) a second order expression is used, e.g., two point central difference, then the expression for boundary values of vorticity would be only accurate to first order.

A problem in implementing the no-slip boundary condition arises in cases where a smooth curve in the physical plane corresponds to a curve with a corner in the computational plane, e.g., in the case of a particle contour. Since there is no physical singularity in the vorticity field at the corners, interpolation is used to determine vortivity values at such points. In the case shown in Fig. 4b the corresponding formula is

$$\omega_{i,j} = \frac{s_{i+1,j}\omega_{i,j-1} + s_{i,j-1}\omega_{i+1,j}}{s_{i+1,j} + s_{i,j-1}}, \tag{33}$$

where

$$s_{i+1,j} = \sqrt{(x_{i+1,j} - x_{i,j})^2 + (y_{i+1,j} - y_{i,j})^2},$$

$$s_{i,j-1} = \sqrt{(x_{i,j-1} - x_{i,j})^2 + (y_{i,j-1} - y_{i,j})^2}.$$

Similar formulas are derived for other corner points.

The solution algorithm for the case of flow in a channel with a particle can now be described step-by-step. Note that as soon as the constant $C$ in (16) is specified the algorithm is essentially that of [16]. Assume that the coordinate grid has already been generated and that the coefficients (9) and (10) are known at every point of the region. First, the constant $C$ in (16) is assigned a value, $C=C_1$. Then an initial approximation for vorticity and stream function is specified at all points inside the region and the values of vorticity on the boundary are calculated from (32) and similar relationships. The equations (28) and (29) can be solved using an

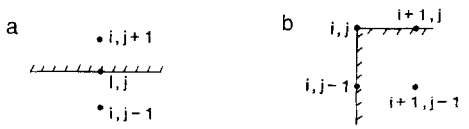


FIG. 4. Boundary points in the transformed plane.

SOR procedure. The overrelaxation factor, $K$, is calculated using the relationship [13].

$$K = 2A((1 - \sqrt{1-\beta})/\beta), \tag{34}$$

where

$$\beta = \frac{1}{4}\left(\cos\frac{\pi}{N_\xi - 1} + \cos\frac{\pi}{N_\eta - 1}\right)^2.$$

$N_\xi$ and $N_\eta$ are the number of points in the $\xi$ and $\eta$ direction, respectively, and the factor $A$ was determined experimentally (close to unity). For the first iteration, $K = 1$ is used since this minimizes the error [15]. For subsequent iterations $K$ is computed from (34). The sweep direction is changed every iteration, and the number of SOR iterations is kept low ($\leqslant 10$) because of the tentative nature of the boundary conditions for vorticity. The computed values of vorticity and stream functions are then smoothed

$$w_{i,j}^{n+1} = w_{i,j}^{n} + k(w_{i,j}^{n+1/2} - w_{i,j}^{n}), \tag{35}$$

where $k$ is the underrelaxation factor; it is set to be 0.7 for vorticity and 0.3 for stream function. Two parameters characterizing the convergence error can be defined:

$$E_1 = \max_{i,j}\left|\frac{\omega_{i,j}^{n+1} - \omega_{i,j}^{n}}{\omega_{i,j}^{n}}\right|, \qquad E_2 = \max_{i,j}\left|\frac{\psi_{i,j}^{n+1} - \psi_{i,j}^{n}}{\psi_{i,j}^{n}}\right|. \tag{36}$$

The outer iteration process is continued until the following convergence criteria are met

$$E_1 < \varepsilon \qquad \text{and} \qquad E_2 < \varepsilon, \tag{37}$$

where $\varepsilon$ is a preassigned parameter taken to be 0.0001. If the criteria (37) are not satisfied the outer iteration is repeated starting with recalculation of the boundary values for vorticity. If the criteria (37) have been met, the integral

$$q = \int_{B_1^*}^{B^*} dp \tag{38}$$

is calculated. The integration contour is shown in Fig. 3b; $B_1^*$ is the beginning and $B^*$ is the end of the integration path $L_p^*$. As was discussed above, $q \neq 0$ for an arbitrary choice of $C$. To determine the value of $C$ which would yield $q = 0$ the described calculations are repeated twice for two different values $C_1$ and $C_2$; the respective values of the integral are $q_1$ and $q_2$. Then, the coefficients in Eq. (19) are determined and the value of $C$ corresponding to $q = 0$ is found from

$$C = C_0 = q_1\frac{C_2 - C_1}{q_1 - q_2} + C_1. \tag{39}$$

Once $C_0$ is determined, the solution $(\psi, \omega)$ is obtained as a linear combination of the solutions $(\psi_1, \omega_1)$ and $(\psi_2, \omega_2)$ corresponding to the constants $C_1$ and $C_2$,

$$\omega = \frac{C_0 - C_1}{C_1 - C_2}\omega_1 + \frac{C_1 - C_0}{C_1 - C_2}\omega_2,$$
$$\psi = \frac{C_0 - C_1}{C_1 - C_2}\psi_1 + \frac{C_1 - C_0}{C_1 - C_2}\psi_2. \tag{40}$$

To complete the solution, the pressure distribution is found from (13), and the force and torque are obtained by computing integrals (20)–(22).

## Sample Applications

The described numerical scheme has been applied to a variety of problems of particle motion in a channel. The detailed results of these studies will be reported elsewhere; here we only present comparisons with the previously known solutions to provide validation of the proposed scheme.

The problem of flow around a circular particle in a plane channel has been investigated in detail; the geometry of the problem is illustrated in Fig. 5. The elements of the resistance matrix $A_{ij}$ in (24) have been calculated for a wide range of particle radius, $R$, and position of the center of the particle in the channel, $y$. Both variables are scaled by the width of the channel; the ranges in our calculations are $0.10 \leqslant R \leqslant 0.45$, $\delta + R \leqslant y \leqslant 1 - \delta - R$, where $\delta$ is the gap between the particle and the wall. The scheme allows accurate calculations when the particle almost touches the channel wall; the smallest gap that we have been able to consider was $\delta = 0.0001$ of channel width. The calculated results cover significantly wider range than previously known solutions [17–19]; the previous solutions were obtained only for axisymmetrically situated particles, $y = 0.5$. Asymptotic expansions in $R$ were used to obtain the analytic solutions, which limited the solutions to the case of relatively small particles, certainly $R < 0.25$.

The horizontal force, $F_{10}$, on a quiescent axisymmetrically situated circular particle in a Poiseuille flow (parabolic velocity profile in the channel far from the particle) was calculated by Faxen [17] in the form of an expansion containing powers of $R$. From the symmetry of the problem it follows that the vertical force, $F_{20}$, and the torque, $T_0$, are equal to zero. Table I lists the values of $F_{10}$ calculated with the

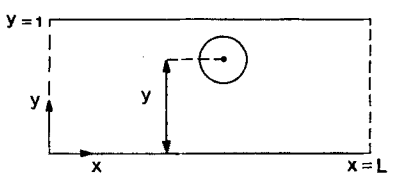


FIG. 5. Geometry of the problem.

TABLE I

Horizontal Force as a Function of Particle Radius on a Quiescent Particle in Poiseuille Flow

| $R$ | Faxen [17] | Present work |
|---|---|---|
| 0.050 | 13.36 | — |
| 0.075 | 18.29 | — |
| 0.100 | 24.31 | 24.08 |
| 0.125 | 31.94 | 31.49 |
| 0.150 | 41.85 | 41.39 |
| 0.075 | 55.00 | 54.27 |
| 0.200 | 72.94 | 71.79 |
| 0.225 | 98.52 | 96.32 |
| 0.250 | 138.5 | 130.8 |
| 0.275 | — | 186.0 |
| 0.300 | — | 259.6 |
| 0.325 | — | 384.4 |
| 0.350 | — | 597.6 |
| 0.375 | — | 996.5 |
| 0.400 | — | 1834 |
| 0.425 | — | 3966 |
| 0.450 | — | 11480 |

help of Faxen's equation [17] for $R \leqslant 0.25$, and the values calculated by the present method for $0.10 \leqslant R \leqslant 0.45$. The accuracy of Faxen's equation is best for small $R$ and deteriorates as $R$ increases; the equation has a singularity at $R = 0.316$ where the force goes to infinity. It is clear, however, that the force must be finite for $R < 0.5$ and increase asymptotically to infinity as $R$ approaches 0.5. To assess the influence of the number of mesh points on the calculated force and torque com-

TABLE II

Calculated Force and Torque on a Quiescent Particle $R = 0.2$ in Poiseuille Flow for Several Different Grids

| | $F_{10}$ | $F_{20}$ | $T_0$ |
|---|---|---|---|
| $N_x = 43$, $N_y = 15$, $N_p = 16$ | 70.73 | 0.0495 | −0.3848 |
| $N_x = 61$, $N_y = 21$, $N_p = 24$ | 71.25 | 0.0015 | 0.0004 |
| $N_x = 73$, $N_y = 25$, $N_p = 32$ | 71.79 | 0.0034 | 0.0005 |
| $N_x = 94$, $N_y = 31$, $N_p = 40$ | 71.88 | 0.0083 | 0.0007 |
| $N_x = 55$, $N_y = 19$, $N_p = 32$ | 73.00 | 0.0330 | −0.2880 |
| $N_x = 61$, $N_y = 21$, $N_p = 32$ | 72.57 | 0.0032 | 0.0006 |
| $N_x = 67$, $N_y = 23$, $N_p = 32$ | 72.10 | 0.0086 | 0.0005 |
| $N_x = 79$, $N_y = 27$, $N_p = 32$ | 71.59 | 0.0047 | 0.0005 |
| $N_x = 85$, $N_y = 29$, $N_p = 32$ | 71.47 | 0.0065 | 0.0006 |
| $N_x = 91$, $N_y = 31$, $N_p = 32$ | 71.41 | 0.0056 | 0.0006 |

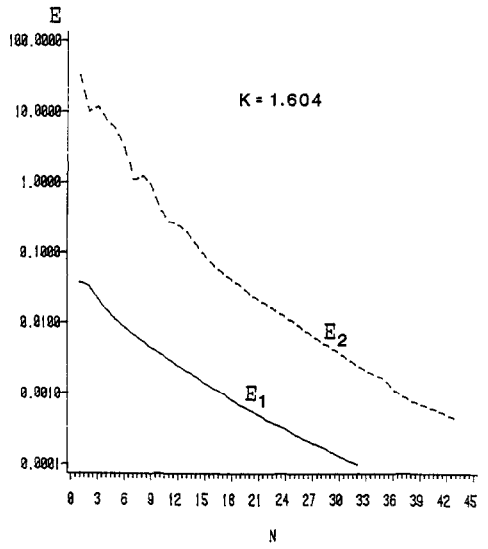


FIG. 6. Convergence history for the case shown on line 3 in Table II.

ponents we conducted a series of numerical experiments. One of them for a fixed geometrical configuration (channel length $L=3$, $R=0.2$, $y=0.5$) is presented in Table II for a variable number of points along the $x$ axis, $N_x$, along the $y$ axis, $N_y$, and on the particle surface, $N_p$. As can be seen from the table, the results are practically independent of the number of points on the boundary. In addition, it can be noted that because we are interested in integral parameters, the possible gain in accuracy per grid node is reduced when the number of nodes is increased due to the necessity of integrating over a larger number of points. The CPU time in seconds required to obtain the first four solutions from Table II on an AS–9000 mainframe computer are 3.16, 4.90, 5.62, and 12.71, respectively. This includes numerical grid generation, computation of vorticity and stream function fields, and calculation of the pressure, forces, and torque on the particle. The over-relaxation parameter was obtained from (34) with $A=0.88$ and is not necessarily optimal for these cases. Figure 6 shows the convergence history for the third case in Table II. This computation was done with the optimal overrelaxation factor, $K=1.604$.

An expression for the horizontal force on an axisymmetrically situated particle translating parallel to the channel walls without rotation was given by Faxen [17] in the form of an expansion containing powers of $R$. As in the preceding case, the expression is valid only for small $R$; it has a singularity at $R=0.313$ where the force becomes infinite. The results from Faxen's equation and the present work are compared in Table III. Note that the force is equal to the coefficient $A_{11}$ in the resistance matrix (24).

The vertical force on a particle translating perpendicular to the channel wall was calculated in [18] using the method similar to [17]. The results are compared with

TABLE III

Horizontal Force as a Function of Particle Radius for a Particle Translating with Unit Velocity Parallel to the Channel Walls

| $R$ | Faxen [17] | Present work |
|---|---|---|
| 0.050 | 8.951 | — |
| 0.075 | 12.33 | — |
| 0.100 | 16.53 | 17.47 |
| 0.125 | 21.96 | 22.81 |
| 0.150 | 29.16 | 30.22 |
| 0.075 | 38.30 | 40.03 |
| 0.200 | 52.57 | 53.72 |
| 0.225 | 72.51 | 73.00 |
| 0.250 | 104.8 | 100.8 |
| 0.275 | — | 145.6 |
| 0.300 | — | 207.8 |
| 0.325 | — | 314.2 |
| 0.350 | — | 500.2 |
| 0.375 | — | 856.9 |
| 0.400 | — | 1621 |
| 0.425 | — | 3607 |
| 0.450 | — | 10760 |

TABLE IV

Vertical Force as a Function of Particle Radius for a Particle Translating with Unit Velocity Perpendicular to the Channel Walls

| $R$ | Westberg [18] | Present work |
|---|---|---|
| 0.050 | 3.712 | — |
| 0.075 | 4.834 | — |
| 0.100 | 6.105 | 6.474 |
| 0.125 | 7.595 | 7.951 |
| 0.150 | 9.380 | 9.830 |
| 0.075 | 11.56 | 12.05 |
| 0.200 | 14.25 | 14.86 |
| 0.225 | 17.63 | 18.27 |
| 0.250 | 21.90 | 22.75 |
| 0.275 | — | 28.52 |
| 0.300 | — | 36.24 |
| 0.325 | — | 46.77 |
| 0.350 | — | 62.52 |
| 0.375 | — | 86.92 |
| 0.400 | — | 127.6 |
| 0.425 | — | 410.0 |
| 0.450 | — | 787.2 |

TABLE V

Torque as a Function of Particle Radius for a Particle Rotating with Unit Angular Velocity

| $R$ | Howland and Knight [19] | Present work |
|---|---|---|
| 0.150 | 0.3042 | 0.3109 |
| 0.200 | 0.5755 | 0.5876 |
| 0.250 | 0.9817 | 1.008 |
| 0.300 | — | 1.649 |
| 0.350 | — | 2.713 |
| 0.400 | — | 4.581 |
| 0.450 | — | 9.008 |

the present numerical solution in Table IV. In this case the force is equal to the coefficient $A_{22}$ in (24).

An analytic solution in the form of infinite series was obtained in [19] for flow around a rotating particle situated in the middle of the channel. The torque on the particle, equal to the coefficient $A_{33}$ of the resistance matrix (24), was calculated for three values of particle radius: $R = 0.15$, 0.20, and 0.25. Table V presents the results of [19] together with the present results.

The calculated hydrodynamic force and torque are integral variables, i.e., they are calculated by integration over the surface of the particle. For additional validation of the numerical scheme it would be desirable to examine a local property of the solution. The following example provides such validation. The flow induced in a closed channel by rotation of the particle represents an example of Stokes flow with closed streamlines. Such flows are of considerable theoretical interest and have been studied by a number of investigators (e.g., [20]). Figure 7 demonstrates the streamline pattern generated by a symmetrically situated rotating particle in a plane channel of length $L = 7$ (note that the results described above were obtained for a channel of length $L = 3$; it was shown that the values of force and torque do not change if the length of the channel is increased). The flow consists of a series of eddies; the velocity in the eddies quickly decreases as the distance from the particle increases. It is interesting to compare these results with the

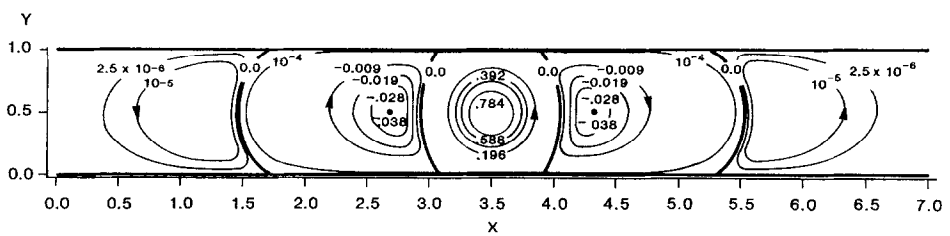


FIG. 7. Streamline pattern for rotation of a particle $R = 0.2$ in a channel of length $L = 7.0$. The values of the stream function are shown.

numerical solution [20] for a rectangular cavity where the fluid motion is generated by the uniform translation of the top wall. It is known [21] that far from the moving wall (i.e., asymptotically) the flow should consist of an infinite set of eddies having length-to-width ratio equal to 1.39. The results in [20] indicate that in the cavity with $L = 5$ this ratio is approached closely in the third eddy from the moving wall . The present result show that for $L = 7$ the first eddy closest to the particle has a length-to-width ratio approximately equal to 1.39.

The calculations were extended to compute all of the coefficients in (24), $A_{11}, \ldots, A_{33}$, $F_{10}$, $F_{20}$, $T_0$ as functions of $R$ and $y$ for Poiseuille and Couette flows. Then Eq. (24) was resolved with respect to translational and angular velocities of a free particle; thus the velocity profiles for the particle center, $U(y)$ and $\Omega(y)$, were calculated for particles of different radii. Also, the case of a particle settling in a vertical channel was considered, and the translational and angular velocity profiles were determined. Finally, an investigation of the motion of a circular particle in bifurcating channels was performed and particle trajectories were calculated using Eq. (26). Some unanswered questions remain. No special treatment has been used for corners in the physical domain. The resulting singularities in the flow variables seemed to be well localized for the cases considered (bifurcating channel) and did not affect the overall flow field. However, it is possible that in severe cases or in cases where the flow near the corner is of interest some special technique may be required. It appears that patching-in an analytical solution in the vicinity of sharp corners should produce good results.

The numerical scheme presented here for creeping two-dimensional flow around particles in a channel of arbitrary shape has extended the results significantly for a number of classical problems (circular particle in a plane channel) and also has obtained the solution where no analytical or numerical results were previously available (particle in a bifurcating channel). The scheme can be applied without any modifications to the motion of noncircular particles. With some minor modifications the scheme can be applied to the motion of multiple interacting particles.

## Acknowledgments

This work was supported by NIH Grants HL 33172, HL-18292, and HL-17421.

## References

1. P. R. Zarda, S. Chien, and R. Skalak, in *Computational Methods for Fluid-Structure Interaction Problems*, edited by T. Belytschko and T. L. Geers, (Amer. Soc. Mech. Engrs. ASME AMD V26, New York, 1977), p. 65.
2. A. Perlin and T. K. Hung, *Eng. Mech.* **104**, 49 (1978).
3. W. E. Pracht, *J. Comput. Phys.* 7, 46 (1971).

4. H. WANG AND R. SKALAK, Office of Naval Research Tech. Report 1, Project NR 062–393, 1967 (unpublished).
5. H. WANG AND R. SKALAK, *J. Fluid Mech.* **38**, 75 (1969).
6. P. GANATOS, R. PFEFFER, AND S. WEINBAUM, *J. Fluid Mech.* **99**, 739 (1980).
7. P. GANATOS, S. WEINBAUM, AND R. PFEFFER, *J. Fluid Mech.* **99**, 755 (1980).
8. P. GANATOS, S. WEINBAUM, AND R. PFEFFER, *J. Fluid Mech.* **124**, 27 (1982).
9. J. F. THOMPSON (Ed.), *Numerical Grid Generation* (North-Holland, Amsterdam, 1982).
10. P. J. ROACHE, *Computational Fluid Dynamics* (Hermosa, Albuquerque, 1976).
11. R. COURANT AND D. HILBERT, *Methods of Mathematical Physics* (Wiley, New York, 1962).
12. A. S. DVINSKY, Ph. D. thesis, Cullen College of Engineering, University of Houston, 1983 (unpublished).
13. J. HAPPEL AND H. BRENNER, *Low Reynolds Number Hydrodynamics* (Prentice–Hall, Englewood Cliffs, N. J., 1965).
14. S. P. FRANKEL, *Math. Tables Other Aids Comput.* **4**, 65 (1950).
15. G. E. FORSYTHE, *Commun. Pure Appl. Math.* **9**, 425 (1956).
16. C. E. PEARSON, *J. Fluid Mech.* **21**, 611 (1965).
17. H. FAXEN, *Proc. Roy. Swedish Inst. Eng. Res.* (*Stockholm*) **187**, 1 (1946).
18. R. WESTBERG, *Proc. Roy. Swedish Inst. Eng. Res.* (*Stockholm*) **197**, 40, (1948).
19. R. C. J. HOWLAND AND R. C. KNIGHT, *Proc. Cambridge Philos. Soc.* **29**, 277 (1933).
20. F. PAN AND A. ACRIVOS, *J. Fluid Mech.* **28**, 643 (1966).
21. H. K. MOFFAT, *J. Fluid Mech.* **18**, 1 (1964).